Desalination and Water Treatment 321 (2025) 100974

Contents lists available at ScienceDirect

Desalination and Water Treatment

journal homepage: www.sciencedirect.com/journal/desalination-and-water-treatment/

Polymeric hydrogels for the removal of fluoride ions from natural water and its toxicity

V. Rosendo-González [a], E. Gutiérrez-Segura [a,*,1], M. Solache-Rios [b], A. Amaya-Chavez [a]

[a] Facultad de Química, Universidad Autónoma del Estado de México, Paseo Colón esq. Paseo Tollocan S/N, Toluca, Estado de México C.P. 50000, Mexico
[b] Departamento de Química, Instituto Nacional de Investigaciones Nucleares, Carretera México-Toluca S/N, La Marquesa, Ocoyoacac, Estado de México C.P. 52750, Mexico

ARTICLE INFO

Keywords:
Drinking water
Fluorides
Hydrogels
Modification
Toxicity bioassays

ABSTRACT

In the present work hydrogels synthetized from polyvinyl alcohol and polyvinyl pyrrolidone (UH) and modified with $FeCl_3$ (MH) were used to remove fluoride ions from natural water in batch and column systems. The natural water used for this work contained 5 mg/L of F^- ions, the maximum permissible limit established by current Mexican regulations is 1.50 mg/L. According to results, the adsorption capacity of the modified hydrogel was higher (MH: 0.342 mg/g) than the unmodified (UH: 0.277 mg/g), based in its application on natural water treatment this value is acceptable; the equilibrium time for MH was 720 min. Three models for each system type (batch and column) were applied, the kinetic data were best fitted to the Ho-McKay model (R^2= 0.993) for batch test and the Clark model for MH in column experiment. The adsorption process was carried out by ionic exchange between the OH^- groups of the adsorbent and the F^- ions. The results of toxicity indices obtained from the bioassay on the seeds reported data in moderate toxicity interval (-2.5 to −0.5) for lettuce and low toxicity (0 to −2.5) for radish with respect to minimum concentrations of F^-. In general, data showed that UH and MH are promising adsorbent materials to remove F^- from natural water and are considered environmentally friendly since they were synthesized with biocompatible materials such as PVA and biodegradable materials such as PVP and citric acid.

1. Introduction

In Mexico and other regions of the world, with high demographic and urban development, the surface water reserve is insufficient to the population and the supply depends on the groundwater, whose quality depends on several factors like the use of the soil and the disposal of waste among other. The chemical composition of groundwater may include the presence of some ions (Na^+, K^+, Ca^{+2}, Mg^{+2}, Cl^-, F^-, HCO_3^-, SO_4^{-2}) due to erosion, solubility of rocks, etc. Currently, it is difficult to extract groundwater with ideal characteristics and therefore it is necessary its treatment.

The properties of groundwater depend on many factors like: weather, landform, geology and biotic factors [1]; during the hydrological cycle, fluoride and other ions dissolve and alter negatively the qualities of the vital liquid. Fluoride in optimal concentrations is essential for the protection of tooth enamel, however, in excessive doses it can be harmful. The fluoride from drinking water, can be absorbed by the mucous membranes, its transport occurs mainly through saliva and breast milk, subsequently is deposited in soft tissues to be incorporated into the bloodstream. Among the adverse health effects that cause concentrations greater than 1.5 mg/L of F^- stand out: gastrointestinal damage, kidney stones, reproductive toxicity due to alterations in the endocrine system, neurotoxicity, cancer, and dental and skeletal fluorosis [2]. The presence of fluoride in water does not impart color, odor, or taste. Therefore, it acts as a latent poison in groundwater [3]. Table 1 shows the maximum permissible limits of F^-, and the corresponding references.

Different processes have been used to treat water with excess of fluoride ions (membrane filtration, precipitation, nanofiltration, ion exchange, electrocoagulation, flotation, reverse osmosis and adsorption among them) [7]. Table 2 summarizes the advantages and disadvantages of the methods used to remove fluoride ions from water, the main

* Corresponding author.
E-mail address: eegutierrezs@uaemex.mx (E. Gutiérrez-Segura).
[1] ORCID ID: 0000–0002-0531–4493

https://doi.org/10.1016/j.dwt.2024.100974
Received 5 October 2024; Received in revised form 20 December 2024; Accepted 22 December 2024
Available online 30 December 2024
1944-3986/© 2024 Published by Elsevier Inc. This is an open access article under the CC BY-NC-ND license (http://creativecommons.org/licenses/by-nc-nd/4.0/).

Table 1
Maximum permissible limits of fluoride ions [2,4–6].

Reference	Maximum permissible limit for F^- (mg/L)	Indicador
NOM−127-SSA1–2021	1.5	Permissible limit for human consumption
WHO, 2022	1.5	Permissible limit for human consumption
EPA, 2009	4.0	Maximum contaminant level guide
China, 2006	1.0	National health standard

Table 2
Conventional techniques for the removal of fluoride ions from water [8–10].

Technique	Advantages	Disadvantages
Coagulation - Precipitation	The process is practical and simpler compared with other defluorination techniques.	Requires high doses of Al $(OH)_3$ (about 700–1200 mg/L) Sludge waste, presence of Al in treated water that can cause Alzheimer's.
Reverse osmosis	Water treatment and purification in a single stage. Guarantees constant water quality. Removes up to 90 % of fluoride ions	Cost A large amount of saline solution is produced. Water becomes acidic and requires pH adjustment. Removes valuable minerals (Mg, K, Ca and Na)
Nanofiltration	The use of chemicals is not required. It represents an effective barrier against suspended solids, inorganic toxins, organic contaminants, pesticides, and microorganisms.	Cost Causes incrustations, peeling or degradation of membranes. Eliminates all ions present in the water.
Electrodialysis	Flexible (seasonal operation) Low demand for chemicals High water recovery.	High energy consumption Possible formation of H_2
Electrocoagulation	It involves the use of basic equipment, easy to handle and with low costs. The water treated with this process is consumable, colorless and odorless.	Hydroxide can re-solubilize. Requires the use of a lot of electricity. The electrodes dissolve during the process due to oxidation
Adsorption	Low-cost, flexibility, easy operation, insensitivity to toxic pollutants, wide pH-range, and high performance	Weak selectivity, waste product, adsorbents require regeneration

disadvantages are high cost, consumption of large amounts of energy and generation of wastes.

Adsorption stands out as a current process in practices focused on the treatment of water contaminated with F^- and that also uses novel materials and represents a relatively low-cost treatment compared to the other techniques already mentioned. Mass transfer from gas or liquid phases (adsorbate) to a solid surface (adsorbent) takes place until the thermodynamic equilibrium is reached, this technique is recognized as a useful method to remove pollutants from water [11]. An important characteristic of adsorption process is the possibility of saturated adsorbent regeneration which reduce the final cost of the process. The objective of the regeneration is return the saturated hydrogel to its original adsorption capacity maintaining its physical, chemical, and structural properties.

There are numerous studies in progress with the main objective of developing new materials or improving the existing ones to use them in the treatment of drinking water. All these results are compiled with the purpose to look for the possibility of using them in large-scale; their advantages over conventional techniques are low cost, environmentally friendly materials, and their possible reuse.

Table 3 shows recent works and methods or procedures focused on the removal of F^- ions from water by adsorption.

Derived from the fact that fluoride ions at concentrations above 1.5 mg/L are harmful, there is a need to evaluate their possible toxicity in living organisms at low concentrations of F^-, the evaluation of acute toxicity, a bioassay was carried out. A bioassay can be dynamic or static, the latter consists of a test that allows the determination of the phytotoxic effects of the remaining solutions after treatments in vegetables such as lettuce and radish, (the seed germination process growth inhibition of the radicle and hypocotyl) with the purpose of determining the level of toxicity of F^- ions during the growth period of the seedlings. The main advantage of using vegetables in phytotoxicity tests is their easy and rapid germination.

The objective of this work is to evaluate the adsorption capacities of fluoride ions by hydrogels based on polyvinyl alcohol (PVA) and polyvinylpyrrolidone (PVP) and the modified one with $FeCl_3$. The adsorption experiments were carried out in batch and continuous systems, using natural water with excess of F^- (4 mg/L); the kinetics, the isotherms and adsorbent regeneration were studied. In addition, the acute toxicity evaluation of F^- in the remaining solutions through a bioassay was determined.

2. Materials and methods

2.1. Materials

Polyvinyl alcohol (PVA: MW 9000–10,000 g/mol, 80 % hydrolyzed) and polyvinyl pyrrolidone (PVP: MW 40,000 g/mol) were purchased from Sigma-Aldrich. Citric acid (CA: MW 192.12 g/mol) and ferric chloride (MW 162.2 g/mol) were supplied from JT Baker. Fluoride standard solution (1000 mg/L) was obtained from Hanna Instruments. All the reagents were of analytical grade.

2.2. Polymeric hydrogels (synthesis and modification)

The adsorbent materials from PVA/PVP polymer mixture were synthesized, cross-linked with citric acid [27], and subsequently modified with $FeCl_3$.

Briefly, 7 g of PVA were put into 100 mL glass flask and mixed with 30 mL of deionized water at 100 rpm until complete hydration was observed. Next, the PVA solution was heated at 93°C to homogenize, then 2.6 g of crosslinker (citric acid) and 2.8 g of PVP were gradually added in this order one after the other until complete dissolution to agglomerations. The temperature was constant at 62°C with constant stirring (150 rpm). Once homogeneity achieved, the mixture was cooled at room temperature and moisture was eliminated for 72 h at room temperature, in the last step the hydrogels were placed into an oven at 130°C for 2 h [28]. The modification of the materials with $FeCl_3$ was done following the method described by Gutiérrez-Segura et al., [29]. The materials were placed in contact with a 0.05 M ferric chloride solution for 24 h. After this time, the hydrogels were recovered by decantation and washed several times with deionized water to remove excess iron. Finally, they were allowed to dry in the same conditions indicated in the synthesis procedure.

2.3. Characterization

Both UH and MH materials were characterized already by different techniques: hydration percentage, point of zero charge (PZC), infrared spectroscopy (FTIR), scanning electron microscopy (SEM), elemental analysis (EDS), thermogravimetric analysis (TGA) and differential scanning calorimetry (DSC). Additionally, adsorbent mass effect and pH of adsorbate solution test were carried out. All these results are reported in a previous paper [28].

Table 3
Recent studies focused on the removal of fluoride ions from water [12–26].

Material	Experimental conditions	Results	Ref.
Co/Fe-LDH@Avocado seed biochar@CMC nanobiosorbent	pH ≤ 2.0 and pH 7.0 100 mg of adsorbent, $C_0 = 5$ mgF^-/L Three water matrices were tested: tap, sea and waste	Adsorption capacity was high. After 105 min, 100 % of F^- was removed in the three matrices	[12]
Aluminum-alginate (AA) foam	$C_0 = 20$ mgF^-/L Room temperature	$Q_{max} = 7.56$ mgF^-/g	[13]
Magnetic La-doped Al_2O_3 core-shell nanoparticle loaded hydrogel beads	Equilibrium time: 24 h Temperature: 298 K Sorbent dosage: 20 mg/g	$q_{max} = 132.3$ mgF^-/g	[14]
Water treatment residues and Fe-modification with iron	pH= 6.5, proposed mechanisms were complexation reaction of F^- with Al^{3+} and Fe^{3+} and ion exchange of F^- with OH^-	q = 6.09 mgF^-/g and q = 16.09 mgF^-/g	[15]
Calcined bauxite	The optimum calcination temperature, dosage and contact time conditions were 400ºC, 40 g/L and 8 min, respectively.	q = 1.05 mgF^-/g	[16]
Silica particles from pumice rock functionalized with iron	The initial concentration was 20 mg/L and optimal pH, sorbent dose and contact time for defluorination were 6, 1 g and 45 min, respectively	Accessible material, low cost and efficient	[17]
Amine-graphene oxide-ferrhydrite (GOUFH)	High specific surface area, due to iron oxide on its surface.	Adsorption capacity of 11.018 mgF^-/g.	[18]
CMC-Ce composite with CeO_2 nanoparticles	Temperature 298 K. This material is an effective adsorbent on removing F^- from water	Adsorption capacity (q_{max}) = 312 mgF^-/g	[19]
Grinded activated alumina	pH= 3.0, C_o= 75 and 100 mg/L	Maximum adsorption capacity: 39 mgF^-/g. The adsorbent can be regenerated to reuse	[20]
Al@ABDC-MOF's and incorporated into CS hybrid beads	Data are not reported	Adsorption capacities, Al@ABDC MOFs and Al@ABDC-CS: 4880 and 4900 mgF^-/Kg, respectively	[21]
Zirconium-Based Composite Nanofiber Membranes (Zr-CNMs)	Adsorption medium tested: acidic and neutral conditions	q = 95 mg/g	[22]
Carboxylated polyacrylonitrile nanofibrous membrane (C-PAN NFM)	The adsorption process is mainly due to chemical adsorption	q = 41.6 mg/g	[23]
Porous MgO nanostructures	Data are not reported	Adsorption capacity was high. After 5 min, 90 % of F^- was eliminated	[24]
Carbon nanotubes stabilized in chitosan sponge	pH 3	q = 975.4 mgF^-/g The material can be reused for at least 5 cycles	[25]
Periclase and lanthanum salt (PC@La nanocomposites)	pH range between 4.0 and 6.0	Adsorption capacity 63.11 mgF^-/g PC@La NC can be regenerated	[26]

2.4. Kinetics and isotherm experiments with natural water

100 mg of each material were put in contact with 10 mL of natural water at pH 6.7 with a fluoride concentration of 4 mg/L at 25°C, 100 rpm and shaking from 0.05 to 72 h.

Different doses of adsorbent (20–400 mg) were used to determine the isotherms at different temperatures (25°C, 35°C and 45°C) and shaking time 72 h.

The concentration of F^- after the adsorption processes was measured using a selective ion electrode, brand, HANNA Instruments HI 4110. Specific quantities of Tissab II and potassium nitrate solution were added to an aliquot of the remaining solution. The calculations were done according to expression reported by Ortega-Aguirre et al. [30], which relates the amount of F^- adsorbed per gram of adsorbent:

$$q_e = \frac{(C_i - C_f)V}{m} \quad (1)$$

where q_e is adsorption capacity of hydrogels, C_i the initial F^- concentration (mg/L), C_f final F^- concentration (mg/L), V is volume (L) and m is mass of adsorbent.

The modified material (MH) was studied in continuous system, because it showed higher adsorption capacity that the unmodified material in the batch system. The flow was 1 mL/min in downward flow; an initial F^- concentration of 4 mg/L; bed height of 20 cm; internal column diameter of 0.7 cm and 5 g of adsorbent (MH) in the column.

2.5. Mathematical models for the batch results

The kinetic models applied were:

Lagergren, also known as pseudo first order model, it is assumed that the adsorption process is of a physical type. According to previous studies, it has been shown that the rate constant does not depend on the concentration [31]. The corresponding equation is described below:

$$\frac{dq}{dt} = k_1(q_e - q_t) \quad (2)$$

where q_t and q_e are the sorption capacities at a time t and at equilibrium, respectively, and whose units are mg/g, k_1 is the pseudo-first-order rate constant, whose unit is 1/min.

Ho-McKay, also called pseudo-second order model assumes that the retention of the species of interest occurs through a chemical process [32]. The mathematical expression is:

$$\frac{dq}{dt} = k_2(q_e - q_t)^2 \quad (3)$$

where k_2 is the pseudo-second order rate constant, whose unit is g/mg*min.

Elovich model assumes that the sorption process is of a chemical type, its application is associated with slow kinetic processes [33], whose equation is:

$$\frac{dq}{dt} = \alpha e^{-\beta q_t} \quad (4)$$

where q_t is the sorption capacity for a time t, whose unit is mg/g, α is the initial sorption rate, expressed in mg/g*min, and β is the surface area-related desorption constant and activation energy for chemisorption, whose unit is g/mg.

Intraparticle Diffusion (IPD) or Weber & Morris model, it is assumed that diffusion in the film formed between the aqueous solution and the sorbent is negligible, which is valid if the system is under constant agitation [34]. The equation of the intraparticle diffusion kinetic model is the following:

$$q_t = k_{int} t^{\frac{1}{2}} \quad (5)$$

where q_t is the sorption capacity for a time t (mg/g) and k_{int} is the rate constant of intraparticle diffusion (mg/g*min$^{1/2}$).

The isotherms models used to treat the experimental data were the following:

Langmuir model assumes the homogeneity of the adsorbent surface, indicating that when the active sites are occupied, adsorption can no longer continue, i.e. there is a saturation in equilibrium. The Langmuir isotherm equation is described below:

$$q_e = \frac{q_0 K_L C_e}{1 + K_L C_e} \tag{6}$$

where q_e is equilibrium adsorption capacity (mg/g), C_e the concentration of F^- in the liquid phase once equilibrium has been reached (mg/L), K_L is the constant related to the affinity of F^- to the binding sites of the adsorbent; Langmuir constant (L/mg) [35], and q_0 represents the maximum sorption capacity in the monolayer (mg/g). q_e and C_e have the same meaning and retain the same units in each of the models mentioned.

Freundlich model assumes that the adsorbent surface is not saturated and that the adsorption energy decreases exponentially as the surface area covered by the adsorbate increases [36]. The Freundlich isotherm equation can be described as follows:

$$q_e = K_F C_e^{\frac{1}{n}} \tag{7}$$

where K_F is the equilibrium constant (mg/g), n is the affinity constant that describes adsorption intensity 1/n (g/L).

Langmuir – Freundlich (Sips), this model predicts heterogeneous adsorption systems.

$$q_e = \frac{a K_{LF} C_e^n}{K_{LF} C_e^n} \tag{8}$$

The model is a combination of the Langmuir and Freundlich models, a is the maximum adsorption, K_{LF} is the mean bonding energy (L/mg)^n and n is related to the degree of heterogeneity of the adsorbent for L-F model [37].

Temkin model is derived, from the Langmuir isotherm. The adsorption energy decreases linearly as the adsorbent surface is covered the adsorbate increases [38]. The Temkin isotherm equation is:

$$q_e = \left(\frac{RT}{b}\right) \ln A C_e \tag{9}$$

where b is the Temkin constant related to heat of sorption (J/mol), A is the Temkin isotherm constant (L/g), R is the gas constant (8.314 J/mol K), and T is the absolute temperature (K).

2.6. Mathematical models for the column system

The mathematical model used to treat the experimental data from the column experiments and to determine the physicochemical parameters of the processes were:

2.6.1. Thomas model

It is used to determine the maximum adsorption capacity of an adsorbent and the theoretical efficiency of the column [39]. The corresponding equation is:

$$\frac{C}{C_0} = \frac{1}{(1 + e^{\frac{K_{th}}{Q}})(q_0 m_B - C_0 V_{ef})} \tag{10}$$

where C is the concentration of the solute at time t (mg/L) and C_o is the initial concentration of the solute (mg/L) K_{th} is the rate constant (mg/min*mg), q_o is the adsorption constant (mg/g), m_B is the mass of the adsorbent (mg), V_{ef} is the volume of the effluent (mL) and Q is the flow (mL min). C and C_0 have the same meaning and retain the same units in each of the models mentioned.

2.6.2. Yoon-Nelson model

The model assumes that the decrease in the probability of adsorption of the molecules present in the adsorbate depends on the adsorption capacity and the advance of the adsorbate through the adsorbent [40]. The expression for this model is:

$$\frac{C}{C_0} = \frac{e^{(K_{YN}t - \tau K_{YN})}}{(1 + e^{K_{YN}t - \tau K_{YN}})} \tag{11}$$

where K_{YN} is the constant of Yoon-Nelson (L/min), τ is the time where $C/C_o = 0.5$ (min), t is the time (min).

2.6.3. Clark model

The mass transfer coefficient in combination with the Freundlich isotherm are used to define a new relationship for the breakthrough curve. The equation is:

$$\frac{C}{C_0} = \left[\frac{1}{(1 + Ae^{-rt})}\right]^{\frac{1}{n-1}} \tag{12}$$

where n, A and r are the constants of Freundlich and Clark [41], respectively.

2.7. Regeneration

The regeneration of both hydrogels (MH and UH) was done in the batch system using NaOH and HCl solutions as regenerating agents. 0.1 g of hydrogel was placed in contact with 10 mL of natural water (4 mg/L of F^-) and kept under constant stirring at 100 rpm, the contact times were 8 and 24 h for MH and UH respectively, considering the equilibrium times from a previous kinetics experiment. Once the adsorbents were saturated with F^-, the adsorbents were placed in contact with the regenerating solutions for 45 min. The concentrations of fluoride ions in natural water were measured before and after the saturation of the hydrogels. Three saturation-regeneration cycles were performed.

2.8. Toxicity bioassay

The quality tests of lettuce (*Lactuca sativa*) and radish (*Raphanus sativus*) seeds were carried out. The minimum germination percentage in this test should be 99 % [42]. The quality test provide data on the germination percentage such as the homogeneity of the seeds and their purity.

Twenty seeds of each vegetable were sown in 100 mm Petri dishes with a 90 mm filter paper, moistened with 5 mL of deionized water. The Petri dishes were placed in the incubator at a temperature of 25ºC for five days and the germinated seeds were counted. The test was performed in duplicate.

Once the quality of the seeds was confirmed, static bioassays were carried out to determine the acute toxicity, of F^- solution after contact with the hydrogels, on lettuce and radish seeds.

Deionized water and an aqueous solution of fluoride ions at different concentrations were used as negative and positive controls respectively. Petri dishes containing the seeds (samples) were impregnated with F^- remaining solutions after treatment with hydrogels (100 %, 50 % and 25 % of its final concentration after the adsorption process), subsequently controls and samples were stored at 25°C for 5 days. Measurements of the length of the radicle and hypocotyl were done with the help of a previously calibrated digital Vernier. The normalized residual germination index (SG) is expressed as a percentage with respect to the control, in addition, the normalized residual elongation of the radicle (RE) and hypocotyl (HE) were determined statistically using Eqs. 13, 14 and 15, respectively [43]:

$$SG = \frac{Germ_{sample(i)} - Germ_{control}}{Germ_{control}} \quad (13)$$

where:

$Germ_{sample(i)}$= Total seeds germinated in F^- solution

$Germ_{control}$= Total seeds germinated in deionized water

$$RE = \frac{Relong_{sample(i)} - Relong_{control}}{Relong_{control}} \quad (14)$$

where:

$Relong_{sample(i)}$= Residual elongation radicle in F^- solution (mm)

$Relong_{control}$= Residual elongation radicle in deionized water (mm)

$$HE = \frac{Helong_{sample(i)} - Helong_{control}}{Helong_{control}} \quad (15)$$

where:

$Helong_{sample(i)}$= Residual elongation hypocotyl in F^- solution (mm)

$Helong_{control}$= Residual elongation hypocotyl in deionized water (mm)

A toxicity scale is classified into four categories depending on the level of damage of an agent towards seedlings: low toxicity (0 to −0.25), moderate toxicity (-0.25 to −0.5), high toxicity (-0.5 to −0.75) and very high toxicity (-0.75 to −1.0) [44,45]. Additionally, the qualitative evaluation of the seedlings was done, 98 % of seeds germinated during the experimental time.

2.9. Statistical analysis

A non-linear multivariate analysis of 96 experimental samples was used, including data fitting to non-linear theoretical models for the evaluation of the adsorption kinetics and isotherms of F^- by the modified and unmodified hydrogels (MH and UH) using the Origin 8.6 software. A numeric analysis was also carried out, from a simple linear regression, to estimate and predict the data of the equation that represents the behavior of the thermodynamic parameters of the adsorption process.

To carry out the statistical analysis for the bioassay of lettuce and radish seedlings, an analysis of variance (ANOVA) was performed, assigning as factors the relationship between lettuce and radish seedlings, germinated in residual F^- solutions at different concentrations, and the germination index (SG), radicle elongation (RE) and hypocotyl elongation (HE) were assigned as response variables. The differences of the variables were assumed through Duncan's multiple comparison test ($\alpha = 0.05$). The numerical analysis was performed with the statistical package corresponding to the analysis of variance used by the Origin 8.6 software. This analysis allowed the evaluation of the toxic effect of the aqueous solution of F^- after the adsorption process.

3. Results and discussion

3.1. Analysis of natural water

Table 4 shows the physicochemical analysis of the natural water, only the fluoride concentration exceeds the permissible limit established in the NOM-127-SSA1–2021, the other parameters are within the norm.

3.2. Adsorption kinetics

Fig. 1 shows the kinetics adsorption behavior of fluoride ions by UH and MH, the equilibria were reached in 24 and 8 h, respectively, iron-modified hydrogel showed higher removal capacity than the unmodified one. The behavior was similar with the results described in a previous work with aqueous solutions of F^-. The iron present in MH is responsible for the increase of the adsorption capacity of the modified material. The presence of hydroxyl ions in the hydrogels structure,

Table 4
Physicochemical analysis of the natural water from Ojocaliente Zacatecas.

Parameter	Ojocaliente Zacatecas (mg/L)	NOM-127-SSA1-2021 Permissible limit (mg/L)
Na^+	56.08 ± 0.02	-
Mg^{+2}	9.36 ± 0.05	-
K^+	7.70 ± 0.05	-
Ca^{+2}	4.59 ± 0.27	-
Cl^-	14.0 ± 0.01	
F^-	4.01 ± 0.08	1.50
SO_4^{-2}	30.70 ± 3.80	400
Total alkalinity	165.3 ± 1.40	-
Acidity	4.00 ± 0.00	-
Total water hardness	128.7 ± 3.50	500
Total dissolved solids	289 ± 10.0	1000

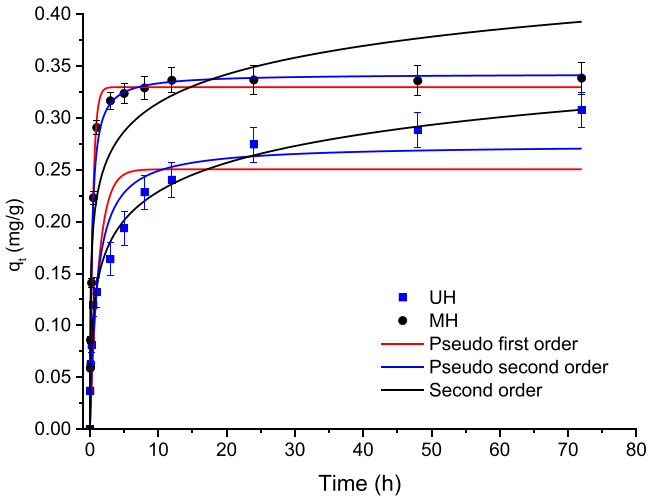

Fig. 1. Adsorption kinetics of F^- from natural drinking water.

promotes ion exchange with the F^- ions. The data were fitted to the second order and pseudo second order models, the results show that the data fit better the second one, indicating chemisorption as the dominant mechanism [46].

The value of q_e= 0.342 mg/g for MH is lower compared to q_e= 0.469 mg/g, this last value was reported previously for the adsorption of F^- from aqueous solutions by the same material. The decrease of hydrogels adsorption capacity in contact with natural water can be attributed to the presence of ions found in drinking water because they may compete for the adsorption sites of the materials [47].

The parameters calculated from the kinetic data and typical models for UH and MH materials are shown in Table 5. The rate constant (K) is greater for MH than UH; the MH reaches equilibrium in the adsorption of F^- process more quickly than UH. Furthermore, the calculated q_e values are similar to the experimental q_e values and the correlation coefficients are high. These results suggest that chemisorption is the main mechanism in the adsorption process of F^- by these materials [48]. Mani et al. [49], reported similar results for the adsorption of fluoride ions with Fe(III) impregnated PVA-based hydrogel beads.

Intraparticle diffusion model also was evaluated, the data adjustment reveals that in the adsorption process two stages are involved: the first step corresponds to rapid adsorption of F^- on the external surface of the adsorbent followed by the diffusion of F^- from the adsorbate to the internal sites of the adsorbent as second step. These mechanisms could occur simultaneously during adsorption. The experimental data did not obey a linear trend and did not cross the origin (Fig. 2), pointing out that both intraparticle diffusion and external diffusion are part of the phenomena that control the F^- adsorption process for UH and MH but also the process involves other mechanisms. Garnica-Palafox et al. [50],

Table 5
Kinetic parameters of F^- adsorption in natural drinking water by UH and MH.

Sample	Lagergren (Pseudo first order)			Elovich			Ho-McKay (Pseudo second order)			Experimental
	q_e (mg/g)	K_L (1/h)	R^2	a (mg/g*h)	b (g/mg)	R^2	q_e (mg/g)	K_2 (g/mg*h)	R^2	q_e (mg/g)
UH	0.250	0.781	0.838	1.208	24.952	0.992	0.274	3.586	0.923	0.278 ± 0.002
MH	0.329	2.381	0.989	10.94	25.202	0.885	0.342	10.717	0.993	0.337 ± 0.006

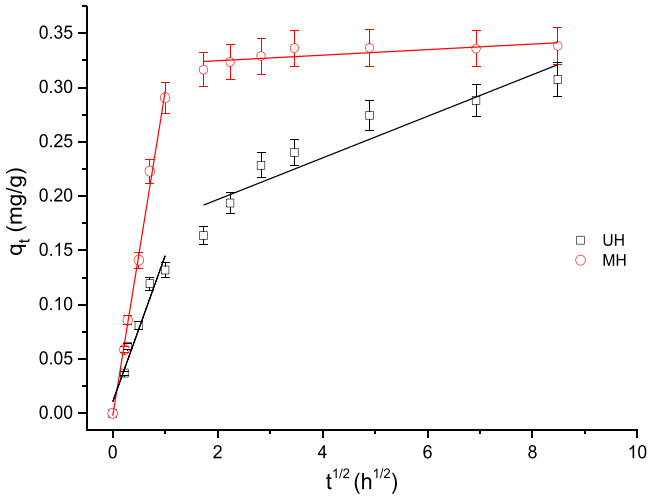

Fig. 2. Adsorption kinetic data of F^- from natural drinking water fitted to the intraparticle diffusion model.

found the same behavior in adsorption studies with CS/PVA Hybrid Hydrogels.

According to results from Table 6 for both hydrogels, k_{dif} of the first step was major than k_{dif} of the second step, this means that the speed in the first stage was faster. C values showed an inverse behavior with respect to k_{dif}; in the first stage; C was minor than in the final stage, i. e, the thickness of the boundary layer in the first stage presented greater opposition than during the second stage, this last had a large duration as a result of a slower speed. The presence of two steps with different diffusion velocities is characteristic of microporous materials [51].

3.3. Adsorption isotherms

The results from the experimental data and their adjustment to the isotherm models can be summarized in the following points:

The adsorption of F^- decreases as the mass of the adsorbent increases from 20 to 400 mg. This effect is due to the conglomeration of adsorbent particles that cause a decrease in the surface area. [52]. This behavior is similar for both materials (UH and MH) in the temperature range from 25ºC to 45ºC; in an exothermic process the release of the analyte can occur and therefore the decrease in the q_e value [53].

Table 7 shows the parameters of the isotherms calculated from the experimental data and models. The data were best fitted to the Freundlich model with a high correlation coefficient, which means that the materials are heterogeneous and multilayers of the adsorbate on the surface of the adsorbent are formed [54]. The Freundlich constant (K_F), which is proportional to the adsorption capacity. It was found that the Freundlich constant MH for the removal of fluoride ions is three times higher than the Freundlich constant found for the UH. The K_F decrease as the temperature increase for both materials. In general, the values of K_F for the removal of fluoride ions (from natural water) are lower than K_F (from aqueous solution) obtained with data reported in a previous study [28].

The experimental data were adjusted to the Temkin model (Fig. 3); b and A parameters for both hydrogels are positives, this means that the adsorption process is exothermic, and the data does not comply accurate lineal adjustment then although the correlation coefficients are acceptable [55].

According to the information obtained from the data adjustment to Temkin model the energy release coincides with the thermodynamic results which are mentioned in next section.

Table 6
Intraparticle diffusion parameters of F^- adsorption in natural drinking water by UH and MH.

Sample	Intraparticle diffusion model constants			
	Step	k_{dif} (g/mg*min$^{1/2}$)	C (mg/g)	R^2
UH	1	0.135	0.011	0.936
	2	0.019	0.159	0.851
MH	1	0.298	−0.002	0.993
	2	0.002	0.319	0.597

3.4. Thermodynamic parameters

Fig. 4 shows ln (q_e/C_e) vs. 1/T. The equations used to calculate enthalpy, entropy and Gibbs free energy changes are:

$$\Delta G^o = \Delta H^o - T\Delta S^o \quad (16)$$

$$\ln (q_e/C_e) = \Delta S^o/R - \Delta H^o/(RT) \quad (17)$$

where R corresponds to the gas constant (8.314 J·mol/K), T is the temperature in K, and q_e/C_e (L/g) is the quotient from adsorption capacity and concentration in equilibrium at different temperatures. ΔH^o and ΔS^o were calculated from the slope and intercept of the lineal equation (Fig. 4) of ln (q_e/C_e) vs. 1/T [56] for UH and MH, respectively.

Table 8 list the thermodynamic parameters that show the adsorption process of fluoride ions by the polymeric hydrogels was exothermic, irreversible, and spontaneous at low temperature, but not spontaneous at high temperature ($\triangle H^o<0$, $\triangle G^o<0$, $\triangle S^o<0$), [57]. The nature of the adsorption of F^- by UH and MH is based on the release of energy, since ΔH was negative, in addition, the spontaneity of the adsorption is verified by the negative value of ΔG^o, while the negative value of ΔS^o indicates that (F^-) adsorbate ions are distributed with better order on the surface of the hydrogel compared to the randomness that they kept in the aqueous solution [58]. In addition, the negative ΔG^o values are lower than −40 kJ/mol indicating that the predominant process is chemical adsorption [59].

3.5. Column adsorption

Column adsorption studies allow the estimation of the feasibility to scale-up the column system for adsorption processes, this type of experiments is ease and simple in operation. In contrast, batch adsorption allows the determination of data regarding the performance and effectiveness of the adsorbent at equilibrium [60]. In column experiments, the continuous flow of the adsorbate over the adsorbent can be validated, as well as the capacity of the adsorbent [59].

MH was tested in column experiments because it showed higher adsorption capacity than UH in batch system. Fig. 5 shows the adjustments to some models of the experimental data obtained from the column test with water naturally containing F^- ions in contact with MH.

Table 7
Adsorption isotherms parameters of F^- at a) 298 K, b) 308 K and c) 318 K.

Adsorbent	Calculated constants of Freundlich and L–F							
		Freundlich			Langmuir-Freundlich (L-F)			
	T (K)	K_F [mg/g (L/mg)$^{1/n}$]	n	r^2	a (mg/g)	K_{LF} (L/mg)^n	n	r^2
UH	298	0.026	0.317	0.966	0.049	0.498	0.2	0.958
	308	0.013	0.222	0.910	0.024	0.136	0.2	0.895
	318	0.011	0.207	0.968	0.042	0.128	0.4	0.847
MH	298	0.096	0.157	0.956	0.072	0.942	0.34	0.758
	308	0.072	0.144	0.967	0.059	0.723	0.29	0.813
	318	0.060	0.138	0.981	0.086	0.642	0.39	0.735

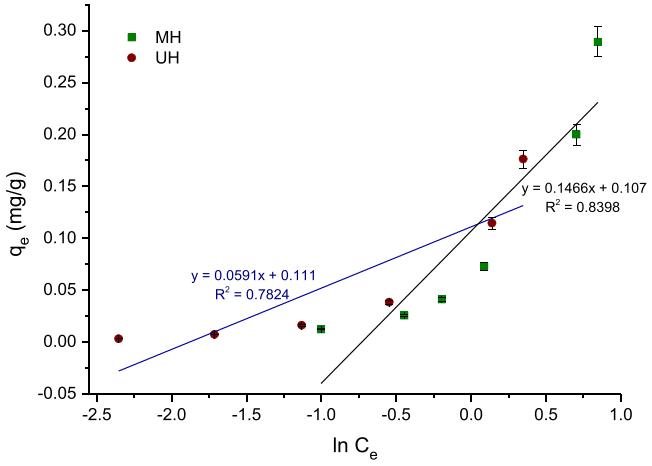

Fig. 3. Adjustment of the experimental data of the adsorption of F^- by MH and UH to the linear isotherm of Temkin at 45ºC.

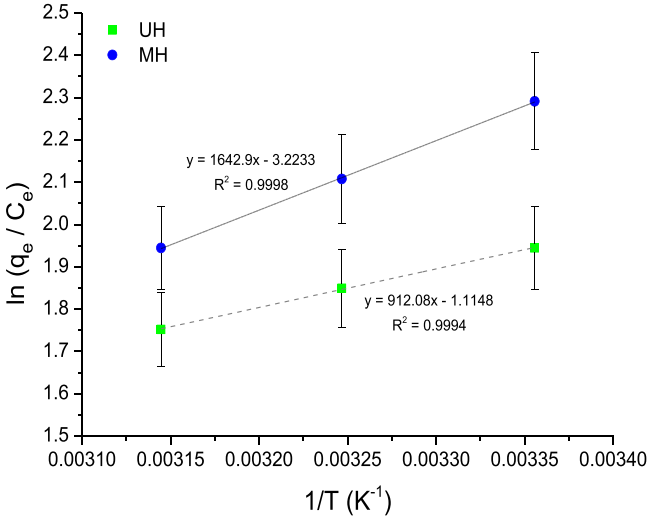

Fig. 4. ln (q_e/C_e) vs. 1/T for F^- on UH and MH.

The parameters from the experimental data and models are shown in Table 9, the experimental data had good fit to the models and the determination coefficients are generally high, the Clark model presented the best fit, that is, the adsorption of adsorbate takes place on a heterogeneous surface. [61]. The adsorption capacity for MH from data and Thomas model was q = 0.304 mg/g. The parameter $K_{\tau/2}$ = 117 minutes of Yoon Nelson model corresponds the time where 50 % of the initial concentration of F^- was retained (q_0 = 0.225 mg/g) and the adsorption capacity at this time was calculate as follows: $q_0 = (C_0{*}Q{*}\tau)/m$ where

Table 8
Thermodynamic parameters of the F^- adsorption processes by the hydrogels.

Material	Parameter	Temperature (K)		
		298	308	318
UH	ΔG° [J/mol]	−4821	−4728	−4636
	ΔS° [J/mol K]		−9.27	
	ΔH° [J/mol]		−7583	
MH	ΔG° [J/mol]	−5673	−5405	−5137
	ΔS° [J/mol K]		−26.80	
	ΔH° [J/mol]		−13659	

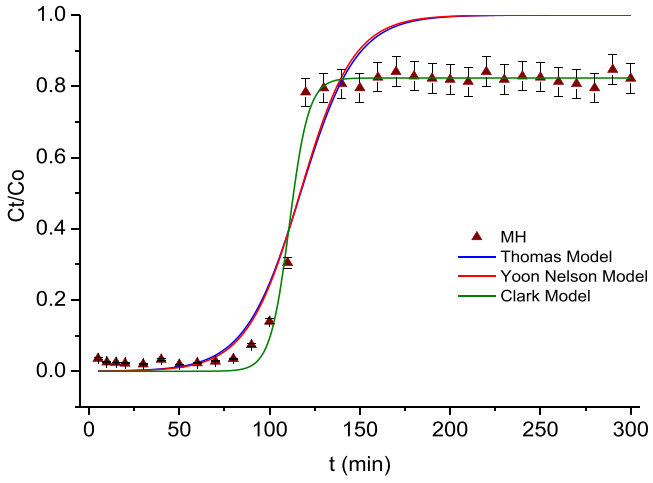

Fig. 5. Column adsorption behavior of F^- by MH from natural drinking water.

q_0 is the adsorption capacity of the column at the breakthrough point (mg/g adsorbent), C_0 is the initial F^- concentration (mg/L), Q corresponds to volumetric flow rate (L/min), τ is the service time (min) obtained when the concentration of the effluent reached 50 % of the influent concentration and m is the mass of adsorbent (g) [62].

Furthermore, Clark model as above mentioned is the one that best fits the breakdown curve, and it indicates that adsorption can occur both on the external surface and in the internal pores of MH. A similar behavior was reported elsewhere Bakhta et al. [63], they studied the removal of fluoride ions using a functional granular adsorbent of aluminum particles incorporated into activated carbon, $Al(OH)_3$@)AC.

3.6. *Regeneration (adsorption-desorption)*

The reuse of the adsorbents is important in adsorption processes [58]. Three adsorption-desorption cycles were carried out on both UH and MH hydrogels, using HCl and NaOH as regenerating agents, the results are shown in Fig. 6. After three adsorption-desorption cycles, the adsorption efficiency values of F^- ions were lower than 80 % of the initial adsorption capacity, regardless of the type of agent and the type of

Table 9
Parameters calculated from the data of continuous flow systems and models.

	Thomas			Yoon-Nelson			Clark			
Material	K_{th} (mL/min*mg)	q (mg/g)	r^2	$K_{\tau/2}$ (min)	K_t (1/min)	r^2	n	K (L/mg)	A	r^2
MH	24.983	0.304	0.901	117	0.068	0.919	0.823	0.187	1.090E9	0.993

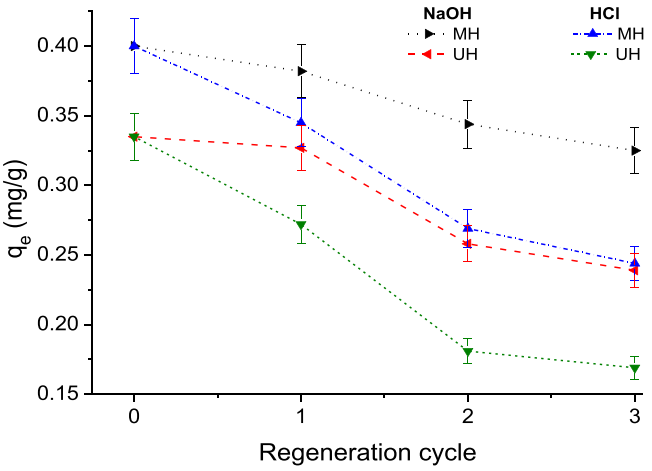

Fig. 6. q_e profile of adsorbents after regeneration.

material, UH or MH. The decrease on removal efficiency is attributed to the slight structural modification that the material may experiences in each cycle; however, this does not affect the feasibility of reusing the hydrogels. It is important to note that the removal in basic medium was higher than in acidic medium in both materials. Wang et al. [64], evaluated the regeneration of an alginate/citrate airgel composite (CA-SC), using HCl and EDTA as regenerating agents and observed that the removal efficiency of the material remained above 80 % after 9 cycles and the change in its structural characteristics was minimal.

3.7. Bioassay

Prior to the bioassay, the quality test of the lettuce "*Lactuca sativa*" and radish "*Raphanus sativus*" seeds was performed, 98 % germinated of both variants, namely, only one seed did not germinate out of 20 seeds of each variant, sown in a petri dish and in duplicate (incubation time: 5 days at 25ºC). It is important to mention that there is currently no literature available on the study of PVA/PVP hydrogels for F^- removal and that also includes acute toxicity tests.

Figs. 8 and 9 correspond to lettuce and radish seedlings, respectively. Three different treatments were carried out from the F^- ion solution which had previous contact with the adsorbent materials: first treatment, solution with initial concentration,Co = 5 mg/L F^-; second and third treatment, solutions with 50 % and 12.5 % with respect to the initial concentration of F^- ions, respectively. Two controls were considered, the positive one corresponds to the growth of the seeds in deionized water that was in contact with the hydrogels, while the negative one belongs to the evaluation of the growth in a F^- solution with the same initial concentration of 5 mg/L without having been in contact with the adsorbents.

Figs. 7 and 8 show considerable growth after the incubation time (5 days) for both lettuce and radish variants. Radish seedlings showed increased growth compared to lettuce seedlings, however, they also exhibited additional characteristics other than size, which are discussed in the next section.

Fig. 9 shows the acceptable percentages of seed germination (SG) for the two variants, the results in both cases were compared with the control. The data obtained were decisive for carrying out the bioassay, since the use of the seed strictly requires a high percentage of germination.

3.8. Qualitative evaluation

3.8.1. Lactuca sativa

In Fig. 10, the treatments with different concentrations of F^- solution tested with both hydrogels (unmodified and modified) are shown. The first group, after the respective controls, corresponds to UH data for the three treatments (12.5 %, 50 % and 100 %), these present less variability in radicle and hypocotyl elongation for *Lactuca sativa* with respect to the second group corresponding to MH whose data show greater variation, around 10 % and 3 % respectively. It is important to mention that for the test with the modified hydrogel in contact with the 100 % treatment of the F^- solution, the results for radicle and hypocotyl elongation showed an increase in growth, exceeding what was recorded for both controls. This may be due to the effect that the F^- ion can cause at an *in vitro* level in some enzymes related to plant cell growth [65], for example, by activating the enzyme isocitrate dehydrogenase (IDH), which is responsible for catalyzing the phases of tricarboxylic acids that are part of the Krebs cycle on which the route for metabolizing energy at the cellular level depends [66].

The mean data depicts the elongation of the parts of the seedling that develop during germination, according to the observations, the

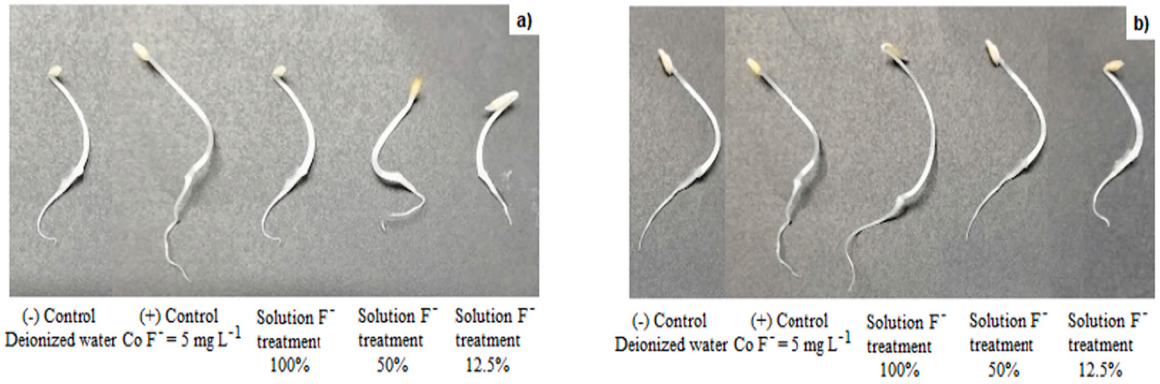

Fig. 7. Growth of *Lactuca sativa* seedlings with F^- solutions treated with: a) UH and b) MH.

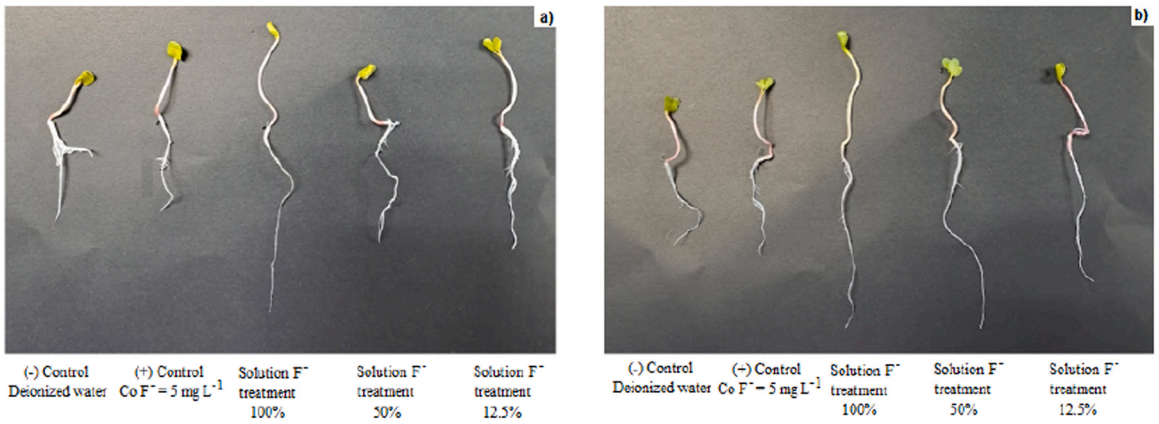

Fig. 8. Growth of *Raphanus sativus* seedlings with F^- solutions treated with: a) UH and b) MH.

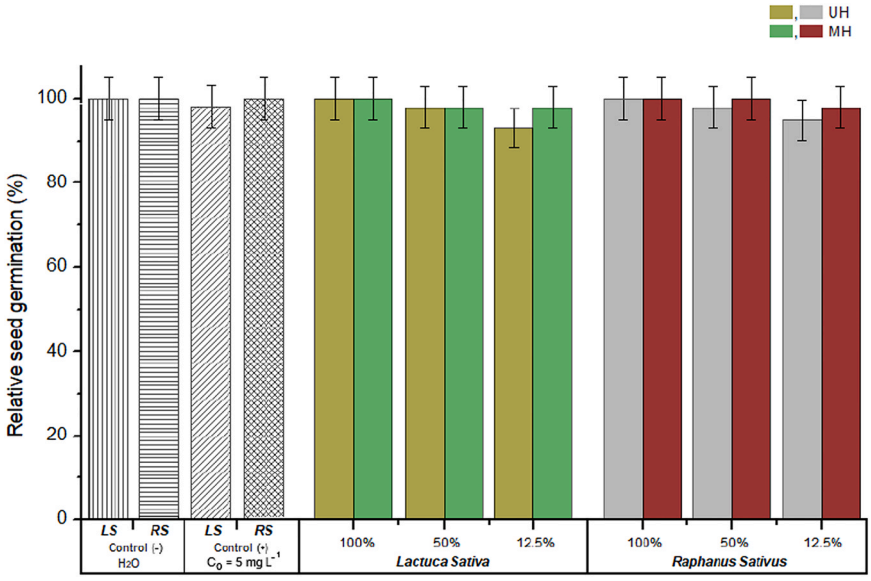

Fig. 9. Percentage of relative seed germination for each concentration of the F^- solution.

seedlings that grew in the treatments with aqueous solutions of F^- that had contact with UH, the radicle showed less elongation (RE) and was visibly thinner, also some presented curling; with respect to the hypocotyl that grew curved, regarding Fig. 7a the cotyledons presented a yellowish color, likewise, the scarce presence of roots was observed in comparison with the seedlings germinated with the treatments of the aqueous solution of F^- after contact with MH. Fig. 7b showed slightly curved hypocotyls and stronger cotyledons, while the presence of roots was abundant.

Almeida et al. [67], carried out a study to identify the effects of KF on the germination and growth of *Lactuca sativa L.* They evaluated different concentrations of KF in an interval between 10 and 30 mg/L for a total time of 40 days. Prolonged exposure reduced the germination rate and root development was observed with those seedlings treated with the highest concentration of KF. There was also a reduction on photosynthesis and therefore lower chlorophyll content, which led to seedlings with leaf tissue in a yellowish-green tone.

3.8.2. *Raphanus sativus*

Fig. 11 shows the results of the treatments (12.5 %, 50 %, 100 %) for *Raphanus sativus* and its respective controls. The variability of the radicle and hypocotyl elongation data for this plant is greater between treatments and sample types compared to the other variant. The greatest growth was observed with the 100 % treatment for radicle elongation for UH and MH, this behavior is similar to the other two treatments in both hydrogels, although with lower data for hypocotyl elongation.

The radish seedling is classified as a hyperaccumulator [68], therefore, it can concentrate traces of the iron present in MH, starting in the radicle, passing through the hypocotyl and reaching the cotyledons, which presented a more intense green tone, as well as a greater elongation of the parts of the seedling. Furthermore, iron is considered a micronutrient responsible for the formation of heme groups that serve as a substrate for the synthesis of phytochrome, which is a photosensitive molecule essential for normal plant photomorphogenesis [69]. This is the main reason for the presence of leaves in radish seedlings after 5 days of the test, these showed an increase the radicle growth, as observed in Fig. 8a, the radicle presented greater elongation, minimal curling and was visibly less thin, namely, the radish seedlings experienced the hormesis effect, which is a phenomenon that produces mild stress, related to premature aging [70] for this variant compared to lettuce seedlings. In general, the seedlings presented well-developed radicles, the control (-) resulted in a growth of lateral roots that did not influence the development of the rest of the vegetative structures and because this sample corresponds to the acute toxicity test of the F^- free hydrogel, it is proven that the materials alone do not produce any effect on the development of the seedlings regardless of the variant. In none of the

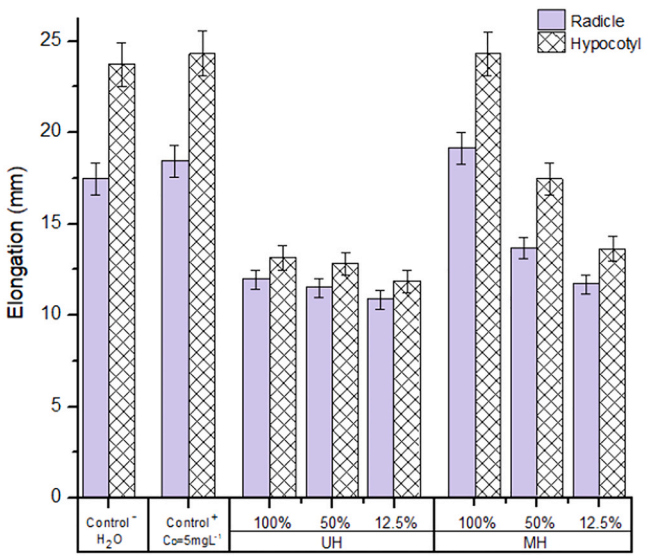

Fig. 10. Mean elongation ± SE (radicle and hypocotyl) of *Lactuca sativa* for: deionized water $C^{(-)}$, F^- solution [5 mg/L] $C^{(+)}$ and treatments at 100 %, 50 % and 12.5 % of F^- remaining solution after contact with UH and MH.

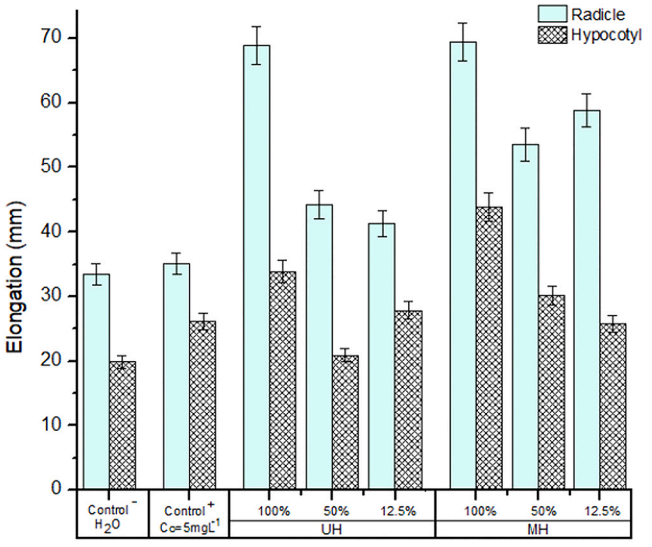

Fig. 11. Mean elongation ± SE (radicle and hypocotyl) of *Raphanus sativus* for: deionized water $C^{(-)}$, F^- solution [5 mg/L] $C^{(+)}$ and treatments at 100 %, 50 % and 12.5 % of F^- remaining solution after contact with UH and MH.

treatments were damages or physiological defects visually evident. The study detailed that the growth of the radicle and hypocotyl of the seedlings under the influence of the treatments with the three different F^- solutions depends on two main factors such as the type of solution remaining from the adsorption process, that is, if it was in contact with UH or MH and the type of vegetable that was used for the test, in summary, according to the results it can be mentioned that the radish seedlings germinated with the MH adsorption solution presented greater elongation. Therefore, based on this behavior, it can be mentioned that *Raphanus sativus* is tolerant to low concentrations of F^- ions (< 5 mg/L), that is, there is a stimulation in the seedling development process caused by traces of contaminant (remaining F^- ions) still present in the solutions that were in contact with UH and MH.

Figs. 12 and 13 categorize the normalized germination rates (SG) as well as the residual elongation levels of the radicle (RE) and hypocotyl (HE) of the bioassays with lettuce and radish seedlings, respectively. As

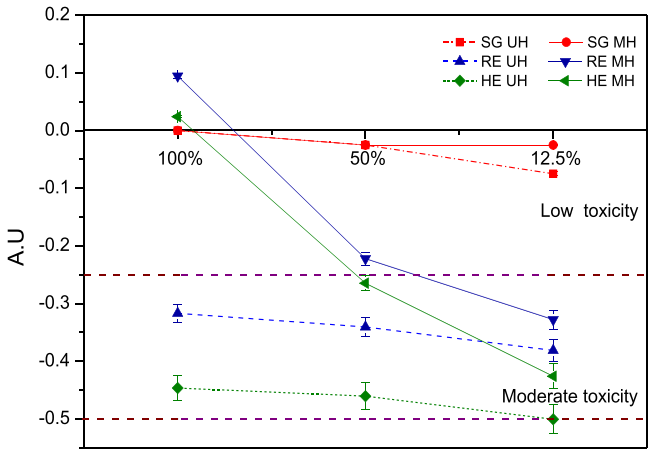

Fig. 12. Toxicity indices for *Lactuca sativa* bioassay ("A.U" = Arbitrary units).

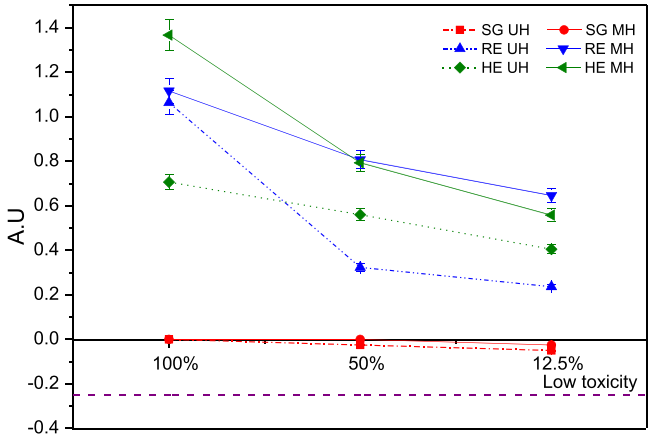

Fig. 13. Toxicity indices for *Raphanus sativus* bioassay ("A.U" = Arbitrary units).

observed in Fig. 12, the SG values for UH and MH and lettuce indicate a low level of toxicity (0 to −2.5) in the three treatments, while the elongation in the radicle and hypocotyl present moderate toxicity levels (-2.5 to −0.5) for lettuce treated with 50 % and 12.5 % of the concentration of the F^- ion solutions after contact with UH, this behavior does not apply to the 100 % treatment after contact with MH because it presented a zero toxicity level ($0.9 > 0$), this means that the growth of the seedling in general is favored. Regarding radish (Fig. 13), a low toxicity level (0 to −2.5) is indicated by the SG values with the three treatments, that is, the morphology of the seedlings was positive for RE and HE ($1.1 > 0$ and $1.35 > 0$), respectively, in all treatments and with greater efficiency compared to the lettuce indices.

4. Conclusion

PVA/PVP-based polymeric hydrogels are good adsorbents for the removal of F^- ions from drinking water in both batch and continuous systems. Kinetic data showed a better fit to the pseudo second-order models (Ho-McKay, R^2=0.993) and the second-order model (Elovich, R^2=0.992) for MH and UH respectively, indicating that the nature of the materials is heterogeneous and that the dominant type of adsorption corresponds to chemisorption. The adsorption capacity of the hydrogels (q=0.342 mg/g) is not high compared to other materials because it depends, among other factors, on the initial concentration of F^-, the objective of this project is based on the treatment of natural water and the adsorption capacity is acceptable for this purpose. Adsorption isotherm data for UH and MH materials were fitted to the Freundlich

model, suggesting that the adsorption process occurs in multilayers on heterogeneous materials. Thermodynamic parameters showed that the adsorption process is exothermic, with spontaneous physisorption at low temperature and predominant, non-reversible chemisorption at room temperature. Regeneration of UH and MH was satisfactory since after three adsorption-desorption cycles the removal percentages in both types of hydrogels exceeded 80 % regardless of the regenerating agent used (acid, HCl or basic, NaOH). It is worth mentioning that after regeneration the hydrogels presented slight changes in their morphology. The feasibility of scaling up the adsorption process using MH for the removal of F^- ions was verified from the column experiment. The data were adjusted to the Thomas, Yoon-Nelson and Clark models, the latter model being the one that presented the best fit of the data, supporting the result obtained from the isotherm experiment in which the best fit corresponds to the Freundlich model that suggests the heterogeneity of the adsorbent. The SG, RE and HE toxicity indices of both seedlings, lettuce and radish showed low to moderate levels of toxicity, in the case of lettuce and with respect to radish the level of toxicity was low; the data for the treatment with 100 % of the F^- concentration for the elongations of radicle and hypocotyl, proved that the presence of iron in MH promotes the development of both parts of the seedlings causing a hormesis effect, accelerating their growth and therefore showing an aging that was not observed in the seedlings germinated with solution in contact with UH. In this way, it can be mentioned that lettuce was more sensitive to the remaining F^- solution compared to radish since it is not considered a hyperaccumulating seedling. Finally, after analyzing the results for the batch and column systems, the effectiveness of polymeric hydrogels for the removal of fluoride ions was verified, acceptable removal percentages of 75 % for unmodified (UH) and 87 % for modified (MH). The application of these materials in the treatment of effluents contaminated with F^- is economical and environmentally friendly compared to other adsorbent materials whose synthesis is more expensive.

CRediT authorship contribution statement

V. Rosendo-Gonzalez: Conceptualization, Investigation, Formal analysis, Methodology and Writing – original draft preparation. **E. Gutierrez-Segura:** Conceptualization, Data curation, Investigation, Methodology, Writing – original draft, Writing – review & editing. **M. Solache-Rios:** Conceptualization, Investigation, Writing – original draft, Writing – review & editing. **A. Amaya-Chavez:** Conceptualization, Methodology, Writing – review & editing.

Declaration of Competing Interest

The authors declare that they have no known competing financial interests or personal relationships that could have appeared to influence the work reported in this paper.

Acknowledgements

V. Rosendo-González is grateful to CONAHCyT for the scholarship. The authors are highly grateful to Universidad Autonoma del Estado de Mexico, UAEMex for the use of laboratory facilities for carrying out the project experiments. We are also thankful to CCIQS and ININ facilities to carry out characterization analysis.

Data availability

Data will be made available on request.

References

[1] Sophocleous M. Interacciones entre aguas subterráneas y superficiales: el estado de la ciencia. J Hydrogeol 2002;10:52–67.
[2] Ahmad S, Singh R, Arfin T, Neeti K. Fluoride contamination, consequences and removal techniques in water: a review. Environ Sci Adv 2022;5:620–61.
[3] Vithanage M, Bhattacharya P. Fluoride in the environment: sources, distribution and defluoridation. Environ Chem Lett 2015;13:131–47.
[4] Solis KF, Saldaña A, Zanor GA, García MG, Saldaña N. Análisis de la capacidad de adsorción de fluoruro en suelo vertisol crómico del estado de Guanajuato y su uso potencial para remediación de aguas. Cs e innovaciÓN Agroaliment 2023;4:99–106.
[5] Bassin EB, Wypij D, Davis RB, Mittleman MA. Age-specific fluoride exposure in drinking water and osteosarcoma (United States). Cancer Causes Control CCC 2006;17:421–8.
[6] Liu S, Liu Y, Wang C, Dang X. The distribution characteristics and human health risks of high- fluorine groundwater in Coastal Plain: a case study in Southern Laizhou Bay, China. Front Environ Sci 2022;10:901637.
[7] Sinha V, Chakma S. Advances in the preparation of hydrogel for wastewater treatment: a concise review. J Environ Chem Eng 2019;7:103295.
[8] Yadav M, Singh G, Jadeja RN. Fluoride contamination in groundwater, impacts and their potential remediation techniques. Groundw Geochem 2021;2:22–35.
[9] Waghmare S, Arfin T. Fluoride removal from water by various techniques: review. Int J Innov Res Sci Eng Technol 2015;2:560–72.
[10] El-Baz A, Hendy I, Dohdoh A, Srour M. Adsorption technique for pollutants removal; current new trends and future challenges - a review. Egyp Int J Eng Sci Technol 2020;32:1–24.
[11] Firdous AD, Swamy K. Recent advances in adsorption techniques for fluoride removal - an overview, Groundw. Sustain Dev 2023;23:101017.
[12] Mahmoud ME, El-Said GF, Almaza ASE, Ghada AAI. Adsorptive capture of fluoride ion from water by Co/Fe-LDH@Avocado kernel seeds biochar@ Caboxymethylcellulose nanobiosorbent: optimization, error function and multivariate analysis. J Ind Eng Chem 2024;133:561–76.
[13] Chang G, Li W, Cao J, Wang Z, Tan X, Wang X. Aluminum alginate foam synthesis, characterization, and application for low concentration fluoride ion removal. Desalin Water Treat 2024;317:100156.
[14] Basu H, Amarnath M, Modak B, Parab H, Basu R, Goyal S, Saha S, Shweta S, Patra CN. Development of magnetic La doped Al_2O_3 core-shell nanoparticle loaded hydrogel for selective recovery of fluoride from aquatic medium. Chemosphere 2024;353:141504.
[15] Ning K, Zheng S, He Y, Hu Y, Hao S, Cui Q, Chen H. Removal of fluoride from aqueous solutions through Fe(III) modified water treatment residues. J Clean Prod 2023;382:135374.
[16] Kimambo V, Ligate FJ, Ijumulana J, Prakash J, Jong R, Ahmad A, Hamisi R, Mtamba J, Mtalo F, Bhattacharya P. Optimization of fluoride removal using calcined bauxite: adsorption isotherms and kinetics. Groundw Sustain Dev 2023; 21:100922.
[17] Kiprono P, Kiptoo J, Nyawade E, Ngumba E. Iron functionalized silica particles as an ingenious sorbent for removal of fluoride from water. Sci Rep 2023;13:8018.
[18] Saldaña-Robles A, Arcibar-Orozco JA, Guerrero-Mosqueda LR, Damian-Ascencio CE, Marquez-Herrera A, Corona M, Gallegos-Muñoz A, Cano-Andrade S. Synthesis of composites for the removal of F^- anions. Nanomater 2023;13:2277.
[19] Ghosh S, Malloum A, Igwegbe A, Ighalo JO, Ahmadi S, Dehghani MH, Othmani A, Gökkuş Ö, Mubarak NM. New generation adsorbents for the removal of fluoride from water and wastewater: a review. J Mol Liq 2022;346:118257.
[20] Kumar R, Sharma P, Yang W, Sillanpää M, Shang J, Bhattacharya P, Vithanage M, Maity JP. State-of-the-art of research progress on adsorptive removal of fluoride-contaminated water environments using biochar-based materials: practical feasibility through reusability and column transport studies. Environ Res 2022; 214:114043.
[21] Jeyaseelan A, Kumar IA, Viswanathan N, Naushad M. Rationally designed and hierarchically structured functionalized aluminium organic frameworks incorporated chitosan hybrid beads for defluoridation of water. Int J Biol Macromol 2022;207:941–51.
[22] Mohamed A, Valadez E, Bogdanova E, Bergfeldt B, Mahmood A, Ostvald R, Hashem T. Efficient fluoride removal from aqueous solution using zirconium-based composite nanofiber. Membranes 2021;11:11020147.
[23] Chen X, Wan C, Yu R, Meng L, Wang D, Chen W, Li L. A novel carboxylated polyacrylonitrile nanofibrous membrane with high adsorption capacity for fluoride removal from water. J Hazard Mater 2021;411:125113.
[24] Borgohain X, Boruah A, Sarma GK, Rashid MH. Rapid and extremely high adsorption performance of porous MgO nanostructures for fluoride removal from water. J Mol Liq 2020;305:112799.
[25] Affonso LN, Marques JL, Lima VVC, Goncalves JO, Barbosa SC, Primel EG, Burgo TAL, Dotto GL, Pinto LAA, Cadaval TRS. Removal of fluoride from fertilizer industry effluent using carbon nanotubes stabilized in chitosan sponge. J Hazard Mater 2020;388:122042.
[26] Kong L, Tian Y, Pang Z, Huang X, Li M, Li N, Zhang J, Zuo W, Li J. Needle-like Mg-La bimetal oxide nanocomposites derived from periclase and lanthanum for cost-effective phosphate and fluoride removal: characterization, performance and mechanism. J Chem Eng 2020;382:122963.
[27] Tekko IA, Chen G, Domínguez-Robles J, Singh R, Hamdan IMN, Vora L, Larrañeta E, McElnay J, McCarthy HO, Rooney M, Donnelly RF. Development and characterization of novel poly (vinyl alcohol)/poly (vinyl pyrrolidone)-based hydrogel-forming microneedle arrays for enhanced and sustained transdermal delivery of methotrexate. Int J Pharm 2020;586:119580.
[28] Rosendo V, Gutiérrez E, Solache M, Amaya A. Removal of fluoride ions from aqueous solutions on unmodified and iron-modified hydrogels. J Polym Res 2024; 31. https://doi.org/10.1007/s10965-024-03954-0.

[29] Gutiérrez E, Solache M, Colín A. Sorption of indigo carmine by a Fe-zeolitic tuff and carbonaceous material from pyrolyzed sewage sludge. J Hazard Mater 2009; 170:1227–35.

[30] Ortega S, Díaz MC, Solache M, Muro C, Alvarado Y, García JJ, Pinedo SY. Effect of alginate on the removal of yellow 6 by a biopolymer-ferric zeolite composite. Sep Purif Technol 2022;292:120971.

[31] Largite L, Pasquier R. A review of the kinetics adsorption models and their application to the adsorption of lead by an activated carbon. ChERD 2016;109: 495–504.

[32] Flores-Alamo N, Solache-Ríos MJ, Gómez-Espinosa RM, García-Gaitán B. Estudio de adsorción competitiva de cobre y zinc en solución acuosa utilizando Q/PVA/ EGDE. Rev Mex Ing QuíM 2015;14:801–11.

[33] Souza TM, Saczk AA, Magriotis ZM, de Sales PF, Resende RF, Pinto FM, Botrel BMC. Kinetic study of the removal of residual copper (II) on activated carbon and alternative adsorbent. J Mech Eng 2015;5:67–71.

[34] Saha B, Orving C. Biosorbents for hexavalent chromium elimination from industrial and municipal effluents. Coord Chem Rev 2010;254:2959–72.

[35] Agarwal AK, Kadu MS, Pandhurnekar CP, Muthreja IL. Langmuir, Freundlich and BET adsorption isotherm studies for zinc ions onto coal fly ash. IJAIEM 2014;3: 64–71.

[36] Baral SS, Das N, Chaudhury GR, Das SN. A preliminary study on the adsorptive removal of Cr (VI) using seaweed, Hydrilla verticillata. J Hazard Mater 2009;171: 358–69.

[37] Jeppu GP, Clement TP. A modified Langmuir-Freundlich isotherm model for simulating pH-dependent adsorption effects. J Contam Hydrol 2012;129:46–53.

[38] Kar S, Equeenuddin SM. Adsorption of hexavalent chromium using natural goethite: isotherm, thermodynamic and kinetic study. J Geol Soc India 2019;93: 285–92.

[39] Yan G, Viraraghavan T, Chen M, New A. Model for heavy metal removal in a biosorption column. Adsorpt Sci Technol 2001;19:25–43.

[40] Pilli SR, Goud VV, Mohanty K. Biosorption of Cr (VI) on immobilized Hydrilla verticillata in a continuous up-low packed bed: prediction of kinetic parameters and breakthrough curves. Desalin Water Treat 2012;50:115–24.

[41] Hu Q, Xie Y, Zhang Z. Modification of breakthrough models in a continuous-flow fixed-bed column: mathematical characteristics of breakthrough curves and rate profiles. Sep Purif Technol 2020;238:116399.

[42] Rajendra S. Testing seed for quality, seed science and technology biology, production, quality. Springer; 2023. p. 299–333. https://doi.org/10.1007/978-981-19-5888-5_13.

[43] Bagur MG, Estepa C, Martín F, Morales S. Toxicity assessment using *Lactuca sativa L.* bioassay of the metalloids As, Cu, Mn, Pb and Zn in soluble-in-water saturated soil extracts from an abandoned mining site. J Soil Sediment 2010;11:281–9.

[44] Hasan M, Mehmood K, Mustafa G, Zafar A, Tariq T, Zassan SG, Loomba S, Zia M, Mazher A, Mahmood N, Shu X. Phytotoxic evaluation of phytosynthesized silver nanoparticles on lettuce. Coatings 2021;11:11020225.

[45] Flores LE, González JV, Carranza MV. Hydrogel applicability for the industrial effluent treatment: a systematic review and bibliometric analysis. Polymers 2023; 15:15112417.

[46] López J, Ramírez LE, Martinez S, Martínez AI, Mijangos OF, González MCA, Carrillo R, Solís FA, Cuevas MC, Vázquez V. Linear and nonlinear kinetic and isotherm adsorption models for arsenic removal by manganese ferrite nanoparticles. SN. Appl Sci 2019;950. https://doi.org/10.1007/s42452-019-0977-3.

[47] Huang L, Yang Z, He Y, Chai L, Yang W, Deng H, Wang H, Chen Y, Crittenden J. Adsorption mechanism for removing different species of fluoride by designing of core-shell boehmite. J Hazard Mater 2020;394:122555.

[48] Tang J, Xiang B, Li Y, Tan T, Zhu Y. Adsorption characteristics and charge transfer kinetics of fluoride in water by different adsorbents. Front Chem 2022;16:917511.

[49] Mani SK, Bhandari R, Nehra A. Self-assembled cylindrical Zr (IV), Fe (III) and Cu (II) impregnated polyvinyl alcohol-based hydrogel beads for real-time application in fluoride removal. Colloids Surf A Physicochem Eng Asp 2020;610:125751.

[50] Garnica IM, Estrella HO, Benítez JA, Sánchez FM. Influence of genipin and multi-walled carbon nanotubes on the dye capture response of CS/PVA hybrid hydrogels. J Polym Environ 2022;30:4690–709.

[51] Simonin JP, Bout J. Intraparticle diffusion-adsorption model to describe liquid/ solid adsorption kinetics. Rev Mex Ing QuíM 2016;15:161–73.

[52] Ghanbari N, Ghafuri H. Preparation of novel Zn–Al layered double hydroxide composite as adsorbent for removal of organophosphorus insecticides from water. Sci Rep Nat Portaf 2023;13:10215.

[53] Van Tran V, Park D, Lee YC. Hydrogel applications for adsorption of contaminants in water and wastewater treatment. Environ Sci Pollut Res 2018;25:24569–99.

[54] Bhaumik R, Mondal NK. Optimizing adsorption of fluoride from water by modified banana peel dust using response surface modelling approach. Appl Water Sci 2016; 6:115–35.

[55] Dada A. Langmuir, Freundlich, Temkin and Dubinin-Radushkevich isotherms studies of equilibrium sorption of Zn^{2+} onto phosphoric acid modified rice husk. IOSR. J Appl Chem 2012;3:38–45.

[56] K.W. Whitten, R.E. Davis, M.L. Peck, G. Stanley, Química, CENGAGE Learning, 10 (2014), ISBN: 978-607-519-958-0.

[57] Wang ZK, Li TT, Peng HK, Ren HT, Lou CW, Lin JH. Preparation and adsorption performance of nano-hydroxyapatite-enhanced acrylamide hydrogel adsorbent. J Polym, Environ 2022;30:2919–27.

[58] Dhumal R, Sadgir P. Bioadsorbents for the removal of salt ions from saline water: a comprehensive review. J Appl Eng Sci 2023;70. https://doi.org/10.1186/s44147-023-00253-1.

[59] Nasiri M, Nezamzadeh A. A comprehensive study on the kinetics and thermodynamic aspects of batch and column removal of Pb(II) by the clinoptilolite–glycine adsorbent. Mater Chem, Phys 2019;240:122142.

[60] Patel I. Comparison of batch and fixed bed column adsorption: a critical review. Int J Environ Sci Technol 2021;19:10409–26.

[61] Sahu N, Bhan C, Singh J. Removal of fluoride from an aqueous solution by batch and column process using activated carbon derived from iron infused Pisum sativum peel: characterization, Isotherm, kinetics study. Environ Eng Res 2021;26: 200241.

[62] Cortés R, Solache M, Martínez V, Alfaro R. Removal of cadmium by natural and surfactant-modified mexican zeolitic rocks in fixed bed columns. Water Air Soil Poll 2008;196:199–210.

[63] Bakhta S, Sadaoui Z, Bouazizi N, Samir B, Cosme J, Allalou O, Le Derf F, Vieillard J. Successful removal of fluoride from aqueous environment using $Al(OH)_3$@AC: column studies and breakthrough curve modeling. RSC Adv 2024;14. https://doi.org/10.1039/d3ra06697e.

[64] Z. Wang Z, Feng Z, Yang L, Wang M. Effective removal of calcium and magnesium ions from water by a novel alginate–citrate composite aerogel. Gels 2021;7: 7030125.

[65] Panda D. Fluoride toxicity stress: physiological and Biochemical consequences on plants. Int J Bio-Res Env Agric Sci 2015;1:70–84.

[66] Adamek E, Góral P, Majnusz K. In vitro and in vivo effects of fluoride ions on enzyme activity. Ann Acad Med Stetin 2005;51:69–85.

[67] Almeida A, Almeida D, Sales JF, Carvalho S, Costa AC, Lino C, Alves da Silva A, Domingos M, Müller C. Morphoanatomical, physiological, and biochemical indicators in *Lactuca sativa* L. germination and growth in response to fluoride. Plants 2022;11:11233406.

[68] Bhardwaj S, Verma T, Raza A, Kapoor D. Silicon and nitric oxide-mediated regulation of growth attributes metabolites and antioxidant defense system of radish (*Raphanus sativus L.*) under arsenic stress. Phyton-Int J Exp Bot 2023;92: 763–82.

[69] Diaz CE, Vallejo W, Cantillo A, Alvis M, Fajardo C. Methylene blue degradation under visible irradiation on TiO_2 electrodessensitized by dye chlorophyll extract from Spinacia oleracea plant. Prospectiva 2018;16:7–12.

[70] Olszyk D, Pfleeger T, Lee EH, Plocher M. Ensayo de fitotoxicidad para la producción de semillas utilizando *Brassica rapa* L. Integr Environ Assess Manag 2010;6:725–34.